

Basic Principles of and Practical Guide to Clinical MRI Radiofrequency Coils

Wingchi E. Kwok, PhD

Abbreviations: RF = radiofrequency, SNR = signal-to-noise ratio

RadioGraphics 2022; 42:898–918

<https://doi.org/10.1148/rg.210110>

Content Codes: **MR** **PH**

From the Department of Imaging Sciences, University of Rochester, 601 Elmwood Ave, Rochester, NY 14642; and University of Rochester Center for Advanced Brain Imaging and Neurophysiology, Rochester, NY. Recipient of a Cum Laude award for an education exhibit at the 2020 RSNA Annual Meeting. Received April 4, 2021; revision requested May 14 and received July 9; accepted August 7. For this journal-based SA-CME activity, the author, editor, and reviewers have disclosed no relevant relationships. **Address correspondence to** the author (e-mail: Edmund_kwok@urmc.rochester.edu).

©RSNA, 2022

SA-CME LEARNING OBJECTIVES

After completing this journal-based SA-CME activity, participants will be able to:

- Describe the RF coil designs commonly used in clinical MRI and the basic anatomy of RF receive coils.
- Discuss proper selection and use of RF coils to achieve optimal image quality, prevent image artifacts, and reduce RF heating risk.
- Explain correct identification of RF coil problems and the methods used in quality assurance of RF coils.

See rsna.org/learning-center-rg.

Radiofrequency (RF) coils are an essential MRI component used for transmission of the RF field to excite nuclear spins and for reception of the MRI signal. They play an important role in image quality in terms of signal-to-noise ratio, signal uniformity, and image resolution. However, they are also associated with potential image artifacts and RF heating that may lead to patient burns. Knowledge of the basic principles of RF coils—including coil designs commonly used in clinical MRI and the anatomy of RF receive coils—facilitates understanding of the use and safety issues of RF coils. Selection of suitable RF coils for individual applications and proper use of RF coils in particular MRI techniques such as parallel imaging are needed to achieve optimal image quality, prevent image artifacts, and reduce the risk of RF burns. The ability to correctly identify RF coil problems and distinguish them from other problems with image artifacts resembling those of RF coil problems allows effective handling of the problems and efficient clinical MRI operation. Quality control of RF coils is required to ensure consistent image quality for clinical MRI and avoid coil problems that may affect image diagnostic evaluation or interrupt patient imaging. There are different phantom test methods for RF coil quality control; the appropriate one to use depends on the coil design and MRI system.

An invited commentary by Ohliger is available online.

Online supplemental material is available for this article.

©RSNA, 2022 • radiographics.rsna.org

Introduction

Radiofrequency (RF) coils are an essential hardware component of MRI. In clinical MRI, they are used for transmission of the RF field to excite proton spins in the body and for reception of MRI signal from the body. RF coils play an important role in MR image quality in terms of signal-to-noise ratio (SNR), signal uniformity, and image resolution. However, RF coils are also associated with potential image artifacts and RF heating that may lead to patient burns.

Appropriate selection and use of RF coils are crucial for achieving optimal image quality while preventing image artifacts and patient burns. Correct identification and handling of coil problems and quality control of RF coils are important to ensure efficient and optimal clinical MRI operation. Therefore, the objective of this article is to provide practical guidance on clinical RF coils to address these issues. The basic principles, proper selection and use, problems and image artifacts, and quality assurance of RF coils used in clinical MRI are discussed to serve as a guide to optimize image quality, prevent image artifacts, and reduce RF heating risk.

TEACHING POINTS

- RF coils play an important role in MR image quality in terms of signal-to-noise ratio (SNR), signal uniformity, and image resolution. However, RF coils are also associated with potential image artifacts and RF heating, which may lead to patient burns.
- RF coil designs commonly encountered in clinical MRI and the basic anatomy of RF receive coils are discussed to provide foundational knowledge for the use and safety issues of RF coils.
- Proper selection and use of RF coils are needed to achieve optimal image quality to maximize diagnostic capability and reduce the risk of RF heating and patient burns.
- The ability to correctly identify RF coil problems and distinguish them from other problems with image artifacts resembling those of RF coil problems allows effective handling of the problems and efficient clinical MRI operation.
- Quality control of RF coils is important to ensure proper functioning of the coils to provide consistent image quality and avoid coil problems that may affect image evaluation or interrupt patient imaging.

Basic Principles of RF Coils

The fundamental components of an MRI system are the magnet, gradient coils, and RF coils. An RF coil is basically a resonant circuit (1). It is tuned to the resonance frequency of proton spins for a given magnetic field (eg, 64 MHz at 1.5 T), similar to a radio tuned to the frequency of a radio station. RF coils may be classified into (a) transmit coils, (b) receive coils, and (c) transmit-receive coils.

During an MRI examination, the transmit coil produces an RF field called the B_1 field, which excites the proton spins and generates a rotating transverse magnetization in the patient's body (Fig 1) (2). The transverse magnetization is then spatially encoded by the magnetic field gradients and detected by the receive coil as an induced voltage signal. A transmit-receive coil serves both purposes: B_1 transmission and signal reception. In this section, RF coil designs commonly encountered in clinical MRI and the basic anatomy of RF receive coils are discussed to provide foundational knowledge for the use and safety issues of RF coils.

Coil Designs

There are many types of RF coil designs, which may be classified from different aspects.

Surface Coils versus Volume Coils.—A *surface coil* is a basic form of RF coil design that typically consists of a single conductive loop (Fig 2A) (1). A surface coil provides strong signal close to the coil, where coupling to the body is stronger; signal decreases with distance from the coil. Smaller surface coils have stronger proximal signal, which drops off faster than that

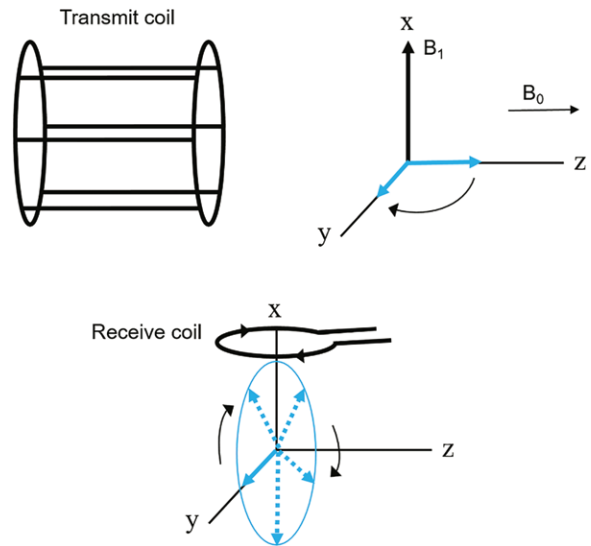


Figure 1. An RF transmit coil generates a B_1 field in the x direction, which flips the proton magnetization from the z-axis (longitudinal magnetization M_z) to the x-y plane (transverse magnetization M_{xy}). The transverse magnetization precesses about the z-axis in the transverse plane and is detected by the receive coil as MRI signal. The induced current in the receive coil is indicated by the arrowheads.

of larger coils (Fig 2B, 2C) (3,4). Moreover, surface coils receive noise only from the sensitive volumes of the coils (noise filtering effect) and thus have higher SNR than volume coils. A surface coil is usually used only as a receive coil and not as a transmit coil, since it produces an inhomogeneous B_1 field, which will cause spatial variation in the RF flip angle, leading to changes in image signal and contrast.

A phased-array coil consists of multiple coil elements, each of which is typically a small surface coil (5–7). The noise-filtering property of surface coils enables a phased-array coil to obtain high SNR as small surface coils (5) while providing a large region of coverage afforded by the multiple elements (Fig 3). However, there are trade-offs to using a larger number of smaller coil elements. First is the higher cost. Second, once the coil element becomes sufficiently small, the resistance from the coil electronics dominates the body resistance, negating many of the noise-filtering effects (5,8). This poses a limit to the maximum number of coil elements, especially for small-array coils.

Another factor to consider is the effect of field strength. Coil resistance and body resistance are proportional to the square root and the square of field strength, respectively (8). Therefore, at higher field strength, the coil resistance is less likely to be the dominant resistance, allowing array coils to have a larger number of elements. Most receive coils nowadays are phased-array coils.

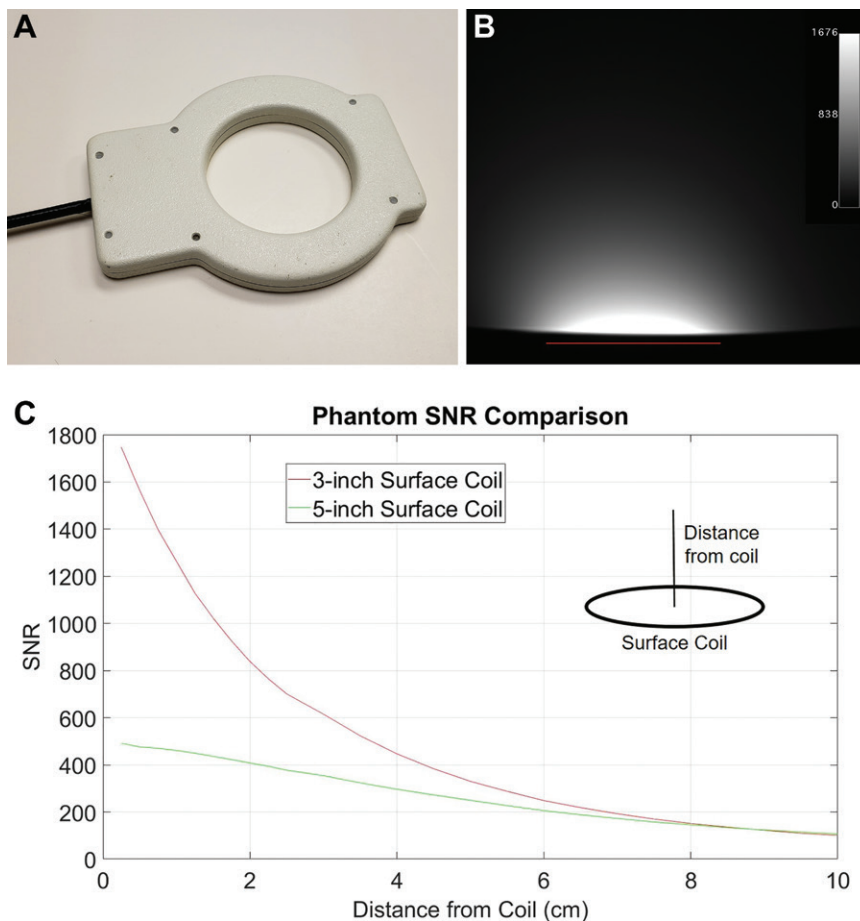
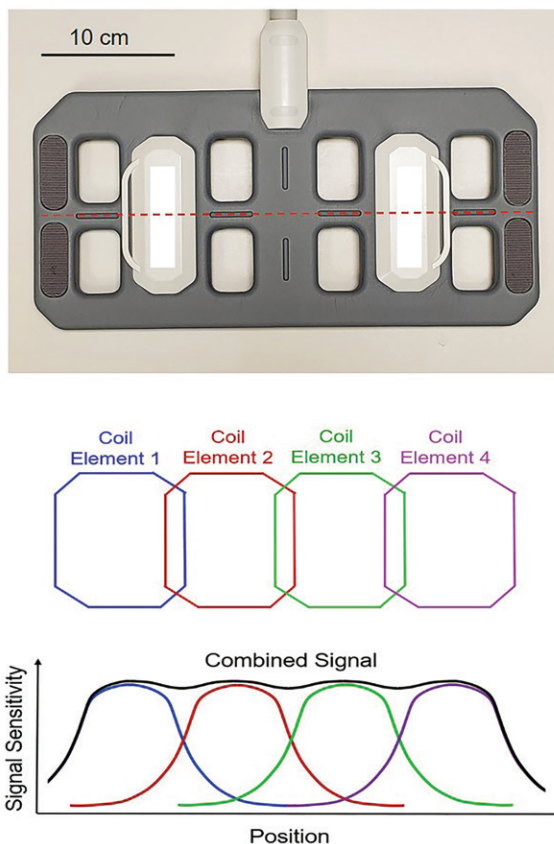


Figure 2. (A) Photograph shows a 3-inch (7.6-cm) surface receive coil. (B) Image of a phantom obtained with the coil, with a red line indicating the position and dimension of the coil. (C) Phantom SNR plots for the 3-inch coil and a 5-inch (12.7-cm) coil, with a diagram showing the SNR values measured along the central axis of the loops.

Figure 3. Photograph (top) and diagram (middle) show a phased-array receive coil with four coil elements. Bottom: The signal sensitivity plots along the midsection of the coil (dashed line in top photograph) show that the phased-array coil possesses the strong signal sensitivity of its small surface coil elements while providing larger spatial coverage.



In the early days of clinical MRI, *volume coils* were typically birdcage coils in design (Fig 4A). They include transmit-receive coils for imaging the head and extremities, as well as the imaging unit body coil, which is often used as an RF transmit coil and sometimes as an RF receive coil. Birdcage coils provide a homogeneous B_1 field and uniform signal reception (9–11). However, they typically provide lower SNR than do other coils (Fig 4C, Fig E1).

While phased-array coils consist of surface coils, many of them have a volumetric geometry, for example, head coils (Fig 4B). Consequently, many phased-array coils can be considered both surface and volume coils. Volume phased-array coils have strong peripheral signal and lower signal in the center (Fig 4C). In volume phased-array coils, the elements are ideally similar in size and distributed evenly to promote uniform and symmetric signal.

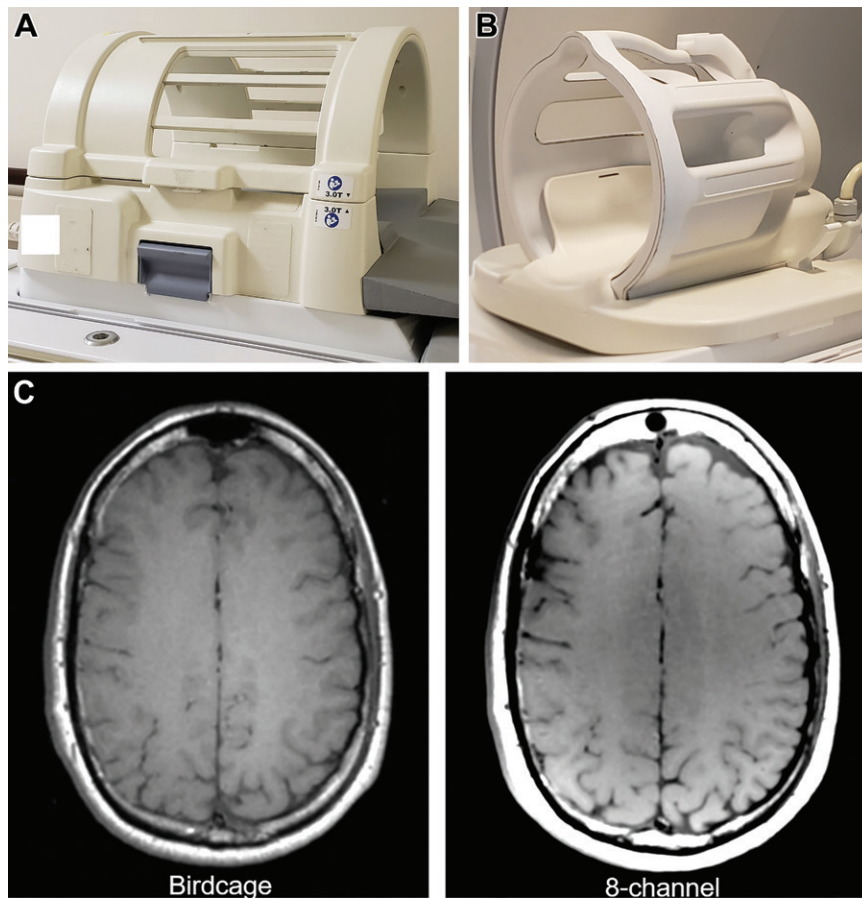


Figure 4. (A, B) Photographs show a birdcage head coil (A) and an eight-channel head coil (B). The elements of the eight-channel coil are distributed symmetrically along the circumference of the coil. (C) Axial T1-weighted spin-echo head images were obtained using a birdcage head coil (left) and an eight-channel head coil (right). The birdcage coil provides more uniform signal but lower SNR than the eight-channel coil.

Local Receive versus Local Transmit-Receive Coils.

While receive coils comprise mostly phased-array coils, local transmit-receive coils include (a) coils that use a birdcage design (eg, head coils [Fig 4A] and early extremity coils) and (b) coils consisting of a birdcage transmit coil and a phased-array receive coil (eg, transmit-receive extremity arrays). For 7-T systems, coils typically have a local separate transmit and receive design because of the lack of a vendor-integrated imaging unit body coil owing to RF power considerations (12,13).

When a local receive coil is used and the imaging unit body coil is used for RF transmission, the B_1 field is present in the entire imaging unit body coil (Fig 5A). In contrast, the B_1 field generated by a local transmit-receive coil is confined to the coil itself (Fig 5B). For example, if a transmit-receive head coil is used for head imaging, there is no need to be concerned about RF power deposition in the abdomen. This information is important for patients with medical implants, as some MRI-conditional implants require use of a local transmit-receive coil away from the implant to avoid exposing the implant to the B_1 field to prevent potential RF heating and burns (14). However, some receive head coils resemble transmit-receive head coils (Fig

6), and care should be taken to ensure correct identification of the coil type.

Linearly Polarized versus Circularly Polarized Coils.

RF coils can also be classified into linearly or circularly polarized coils (15,16). For linearly polarized RF coils, transmission of the B_1 field or reception of the MRI signal is carried out along one axis (Fig 7). The B_1 field in a linearly polarized transmit coil can be viewed as being composed of two counterrotating circular fields: a B_{1+} field in the same direction as the precessing proton spins and a B_{1-} field in the opposite direction. The B_{1+} field is used for spin excitation, while the B_{1-} field is useless.

In contrast, a circularly polarized (or quadrature) transmit coil produces only the B_{1+} field, thus saving half of the transmit power compared with linear polarization (15). Quadrature transmission requires use of two orthogonal RF coil channels to generate two RF fields with the same amplitude but a phase shift of 90° between them. Clinical MR imaging units typically use circularly polarized birdcage coils for RF transmission.

In contrast to linearly polarized receiving, which uses a single coil or channel, circularly polarized receiving (or quadrature detection) requires use of two orthogonal coils or channels

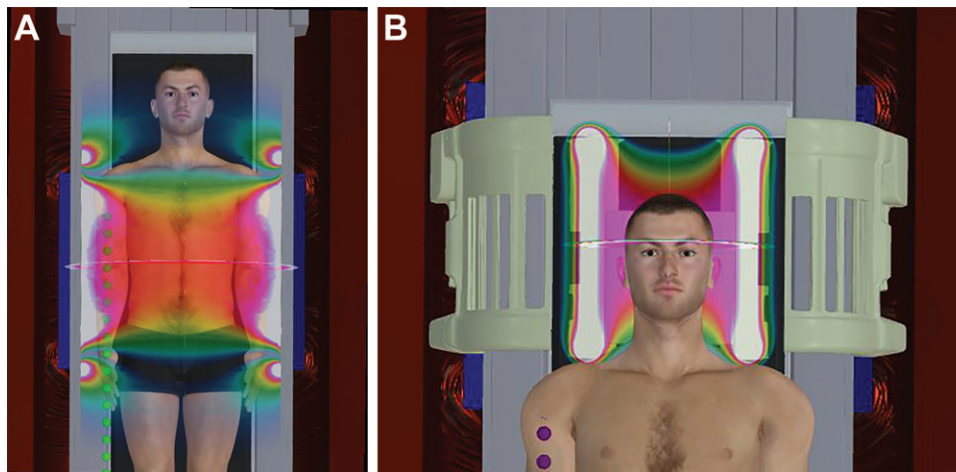


Figure 5. (A) Simulated B_1 field map of an imaging unit body coil shows that the B_1 field is present in the whole body coil. (B) Simulated B_1 field map of a transmit-receive head coil shows that the B_1 field is confined to the local coil. The simulated B_1 field maps were generated using MagnetVision (Advanced Magnetic Analytics).

(Fig 8). The coils provide two signals with uncorrelated noise, which when combined with a 90° relative phase shift produce $\sqrt{2}$ improvement in SNR (15,16). Quadrature detection has been used in birdcage coils such as head or body coils (11) and some older spine coils (17). However, quadrature detection is seldom implemented in newer coils, owing to image shading artifacts associated with quadrature detection in planar-array coils (18) and the increase in coil elements in modern array coils. Nowadays, receive array coils are usually linear coils.

Multitransmit versus Circularly Polarized

Transmit Coils.—The RF wavelength inside the body is greatly reduced from that in free space, owing to the high dielectric constant of the human body. When this is coupled with the fact that RF wavelength is inversely proportional to the magnetic field strength, the wavelength inside the body (about 26 cm at 3 T) may be shorter than the dimensions of the body at 3 T or above. When a circularly polarized transmit coil is used, this will cause interferences in the B_1 field in a phenomenon called standing wave effect (19). The resultant B_1 inhomogeneity can lead to dielectric artifacts, which manifest as image shading inside the body (Fig 9B).

This problem may be mitigated by use of multitransmit coils consisting of independent coil channels (21). By adjusting the phase and magnitude of the B_1 fields for the individual channels, the homogeneity of the B_1 field can be improved to counter the dielectric effect in the body. This process is called B_1 shimming.

In recent years, dual-transmit technology has been available on some clinical MRI systems (20,22,23). It manipulates the two RF transmit

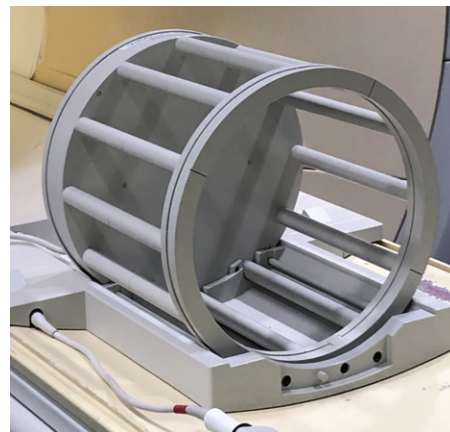


Figure 6. Photograph shows a receive-only head coil, which has a similar appearance to that of a transmit-receive birdcage head coil.

channels in the imaging unit body coil, conventionally used in quadrature mode to provide for B_1 field adjustment (Fig 9). B_1 shimming is particularly useful for large patients and patients with ascites in which there is a large amount of fluid accumulation. A drawback of multitransmit technology is that it may increase local RF power deposition (24) inside the body. Some MRI-conditional metallic implants specify use of only quadrature RF transmission in their MRI safety conditions because of RF heating concerns.

In current clinical 3-T systems, the standard number of transmit elements is two (dual transmit). For 7-T systems, the typical numbers are two to eight, owing to the need to correct for a much stronger dielectric effect (12,13). The challenges of increasing the transmit coil elements include increased complexity of the system, added cost, and increased computational time for RF power deposition calculation (25). The advantages

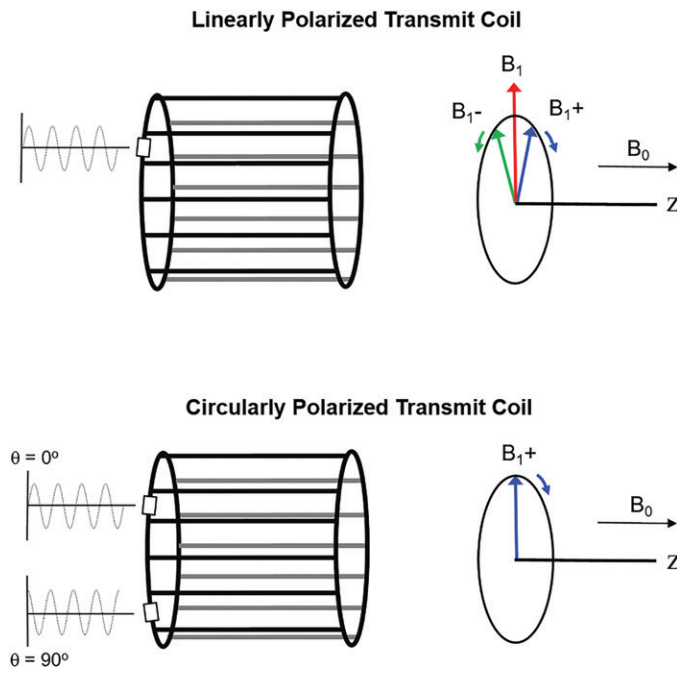


Figure 7. Linearly polarized versus circularly polarized transmit coil. The linearly polarized transmit coil generates a B_1 field along one axis. The B_1 field can be viewed as comprising a B_{1+} field that is used for RF excitation and a B_{1-} field that is useless. In contrast, a circularly polarized transmit coil produces only the B_{1+} field. It requires use of two orthogonal RF transmit coil channels to generate two RF fields with the same amplitude but a phase difference of 90° .

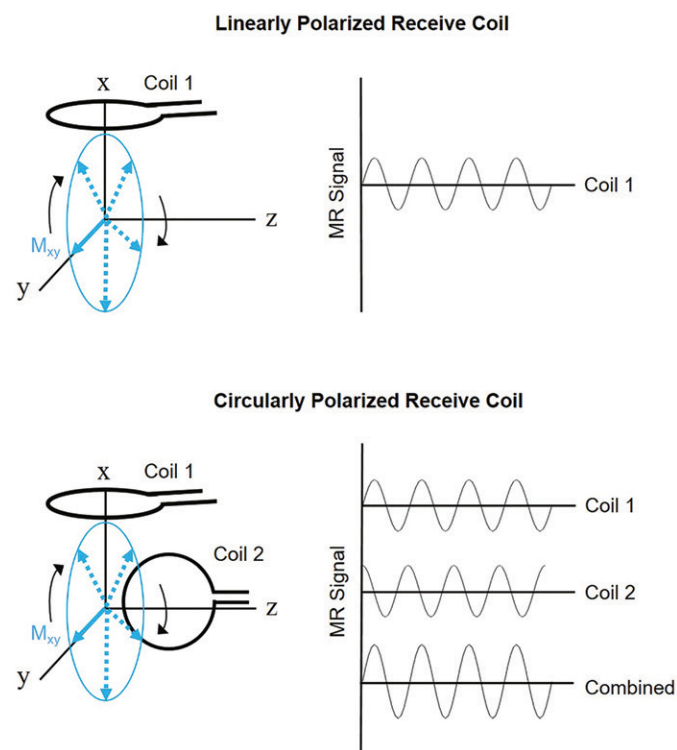


Figure 8. Linearly polarized versus circularly polarized receive coil. The linearly polarized coil detects signal only in the x direction, while the two circularly polarized receive coils detect signal in the x and y directions. The two signals obtained with circular polarization can be combined to give $\sqrt{2}$ improvement in SNR.

are increased degree of adjustment among the coil elements to further improve B_1 homogeneity and reduce RF power (22). While studies show improved B_1 homogeneity with increasing channel count at $3T_1$, the greatest improvement is between single- and dual-transmit coils (22,25).

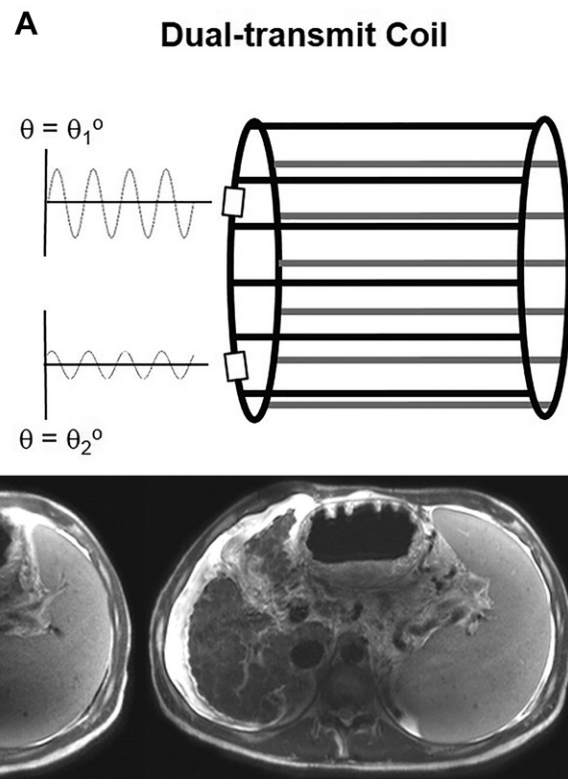
Anatomy of an RF Receive Coil

The basic construction of an RF receive coil consists of the following components (1,7) (Fig 10):

Coil Loop.—The coil loop is typically made of copper wire or tape mounted on a rigid acrylic housing or flexible substrate and may also be a loop etched on a printed circuit board. It is usually circular, oval, or rectangular.

Tuning and Matching Circuitry.—Tuning of the RF coil to the proton resonance frequency is achieved through inductor-capacitor (LC) resonance, where L is the inductance of the coil loop

Figure 9. (A) A dual-transmit coil consists of two independently controlled coil channels to generate two B_1 fields, whose phase θ and amplitude can be independently adjusted to improve the homogeneity of the overall B_1 field to counter the dielectric effect from the body. (B) Axial T2-weighted fast spin-echo images obtained at 3 T with quadrature (left) and dual-transmit (right) RF excitation in a patient with liver cirrhosis and ascites. Both readers in the study assigned the quadrature transmit image a poor score (score = 2), with questionable diagnostic quality due to prominent standing wave artifacts (arrows). They assigned the dual-transmit image a good score (score = 4), with only mild standing wave artifacts. (Reprinted, with permission, from reference 20.)



and C represents the equivalent capacitance in the coil loop circuitry (Fig 10) (1). The coil resonant frequency (f) is given by the following:

$$f = 1/2\pi\sqrt{LC}.$$

Matching is performed to adjust the output impedance of the coil loop terminal to 50 ohms by selecting a proper value for the matching capacitor ($C1$ in Fig 10) to minimize the noise figure of the preamplifier (5,26).

Detuning Circuitry to Decouple from the Transmit Coil.—During MRI, the B_1 field produced by the transmit coil can induce high electric current in the receive coil, causing RF inhomogeneity, which may result in banding image artifact near the coil and overall signal loss (Fig 11). More important, the induced current can generate RF heating, which may lead to coil damage and patient burns. Therefore, each receive coil needs to be decoupled from the transmit coil (7,27–30). This decoupling circuitry is composed of active and passive detuning circuits (Fig 10). The active detuning circuit is activated by DC voltage to forward-bias its diode ($D1$), while the passive detuning circuit is activated by the induced voltage from the B_1 field and serves as backup protection in case the active detuning circuit fails to function.

Preamplifier.—A preamplifier is an electronic component located at the coil loop terminal to

amplify the MRI signal (typically in millivolts) before it is digitized (Fig 10) (7,31). For a phased-array coil, preamplifiers also serve another important purpose of reducing inductive coupling among the coil elements (5). A preamplifier with low input impedance (typically about 2 ohms) forms part of a parallel LC resonance circuit ($L1$, $C1$) to create high impedance to reduce electric current in the coil loop, which in turn reduces the signal coupling and noise voltage transfer among coil elements. This is important, as inductive coupling among coil elements may degrade SNR and also affect parallel imaging performance, especially if data from the elements are not combined using optimum weighting (32–37).

Cable Trap.—Electric current may be induced by the B_1 field on the cable shield of an RF coil or by unbalanced loop voltages coupled to the cable shield in a transmit-receive coil (38). Cable shield current can cause heating in the cable and lead to patient burns (Fig 12). To prevent cable shield current, cable traps are usually installed along the cable of a receive or transmit-receive coil (Fig 13) (38,39). They consist of parallel LC circuitry in the cable shield to block the current (Fig 10).

Selection and Use of RF Coils

Proper selection and use of RF coils are needed to achieve optimal image quality to maximize diagnostic capability and reduce the risk of RF heating and patient burns (40–43).

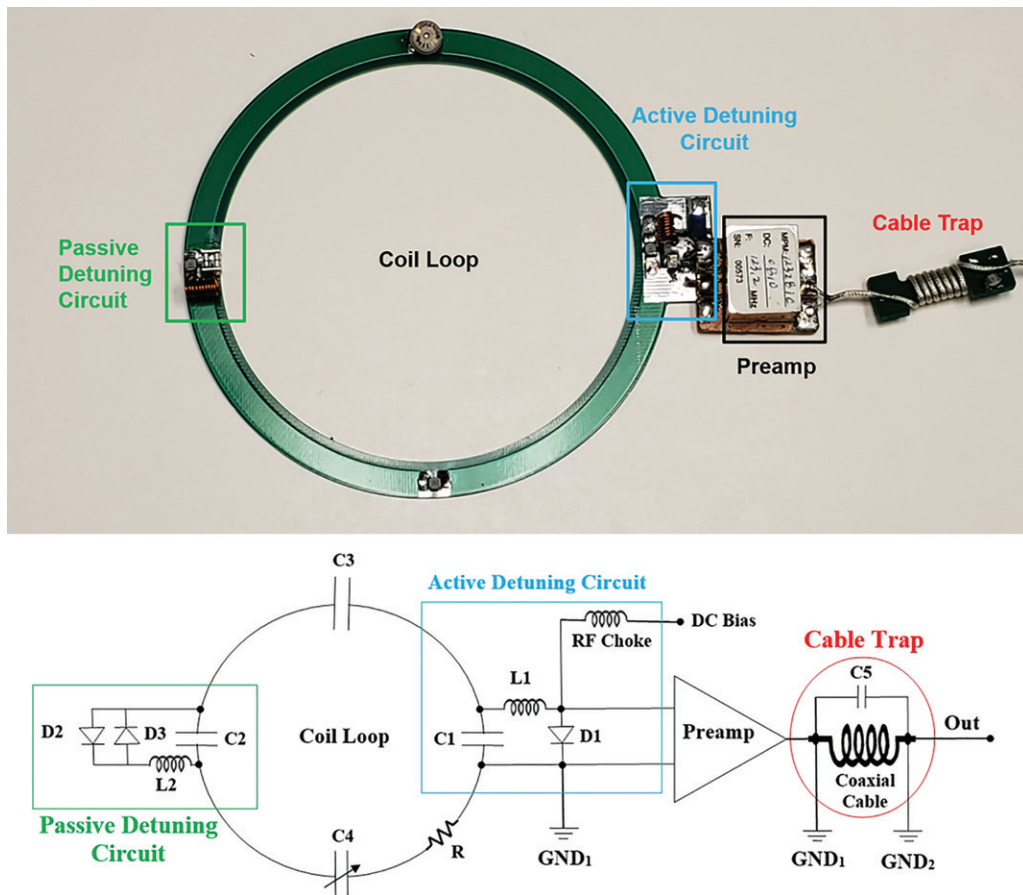


Figure 10. Photograph (top) and diagram (bottom) of the main components of a receive coil show the coil loop, capacitors (C) for tuning (C1–C4) and matching (C1) the coil, detuning circuits for decoupling from the transmit coil, the preamplifier (*preamp*), and the cable trap. *D* = diode, *GND* = ground, *L* = inductor, *R* = resistor.

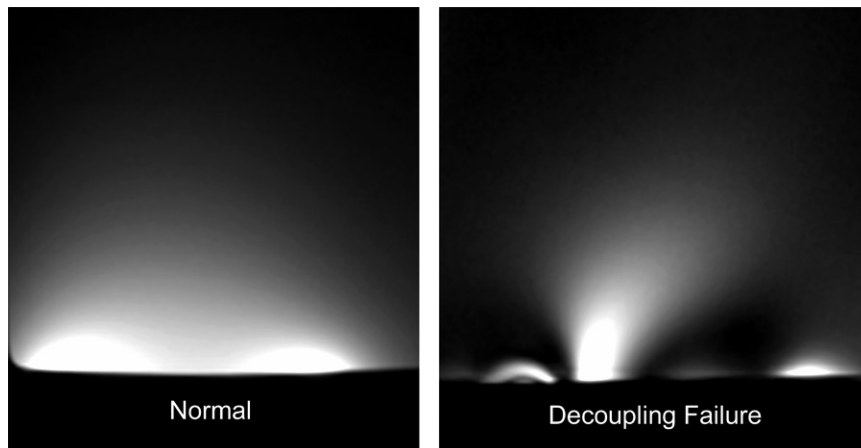


Figure 11. Images of a phantom obtained with a normal coil (left) and a coil that failed to decouple from the transmit coil (right). RF coupling with the transmit coil causes banding image artifact near the coil and overall signal loss.

Selection of RF Coils

Rigid versus Flexible Coils.—Clinical RF receive and transmit-receive coils used to be dominated by rigid coils, which have a hard external casing (Fig 4A, 4B). The casing maintains the shape of the coil and also provides protection to the coil

components. Rigid RF coils are usually designed for specific body parts.

Flexible RF coils have also been used in the clinical MRI community but in recent years are becoming more popular (Fig 14A). They are receive coils that can be used to image a wide range of body parts and are increasingly favored

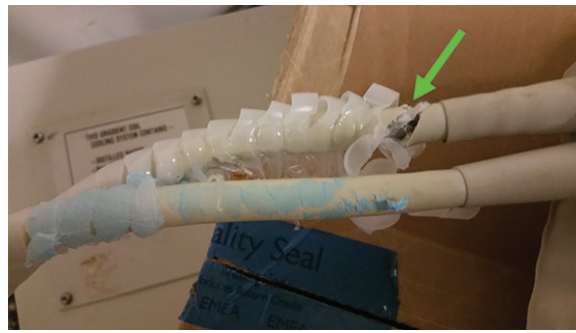


Figure 12. Photograph shows a coil cable that was damaged (arrow) by induced RF heating during MRI. The patient suffered a minor burn on her arm.



Figure 13. Photograph shows cable traps (arrows) along the cable of an RF coil.

over rigid coils dedicated for specific body parts. Use of flexible coils can reduce the number of RF coils needed in an MRI facility. In addition, flexible coils can be wrapped around the imaged body part to provide high SNR (Figs 14C, E2).

However, there are potential issues to consider regarding flexible coils. First, it is generally harder to position and immobilize the imaged body part with flexible coils, which may lead to longer setup time. Second, coupling among coil elements may be significantly increased if the coil is wrapped in a fashion that it is not designed for, leading to lower image SNR (32). Third, images may demonstrate artifacts at locations close to the coil due to metallic components present inside the coil. Fourth, flexible coils are more prone to physical damage.

Emerging Coil Technologies.—Emerging coil technologies include adjustable coils, ultraflexible coils, and coil shimming.

The volume of a rigid coil is typically designed for the general population (7). This causes some coils to be too small in patients with a large or abnormally shaped body part and too large in patients with a small body part to achieve optimal signal sensitivity. To alleviate this problem, *coils with adjustable size* have been developed (Fig 15).

In recent years, *ultraflexible coils* have been developed (44–46). They are lightweight and very flexible coils that can be conformed closely to the patient's contour to increase comfort and optimize SNR (Fig 16C, Fig E3). Among them, coils

made up of linked resonators (Fig 16) (44) have very low coupling among coil elements, enabling the coil to be wrapped in different ways without significant degradation of image quality.

Coil shimming is a newly available technology for improving local B_0 homogeneity by incorporating shim coils within an RF coil (47–49). It is becoming available on commercial MRI systems and is particularly useful for improving imaging quality in the head and neck region (49).

Use of RF Coils

This section discusses some common RF coil application scenarios, in which an understanding of how imaging performance is related to specific coil design and the imaging parameters is required to optimize image quality and prevent image artifacts.

Parallel Imaging.—MRI generally requires long imaging time compared with that of other imaging modalities, owing to the numerous phase-encoding steps in each acquisition. Parallel imaging techniques such as generalized autocalibrating partial parallel acquisition (GRAPPA) (50) and sensitivity encoding (SENSE) (51) reduce imaging time by manipulating spatially dependent information obtained from the individual coil elements of a phased-array coil to reduce the phase-encoding steps (50–54). Parallel imaging can also be used to reduce susceptibility distortion artifacts in echo-planar imaging (EPI) sequences such as diffusion imaging and functional

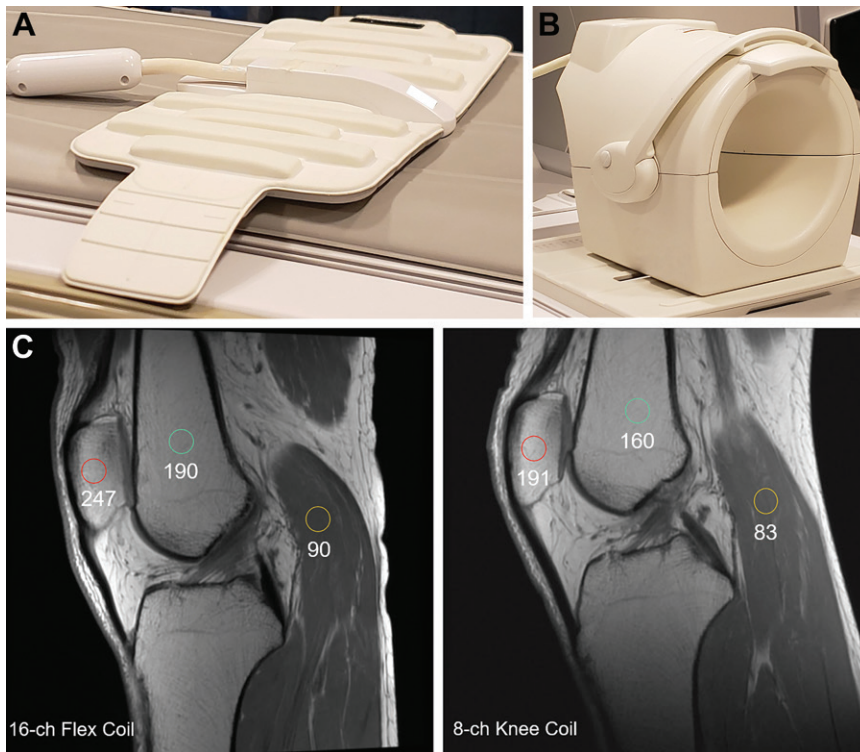


Figure 14. (A, B) Photographs show a 16-channel flexible coil (A) and an eight-channel knee coil (B). (C) Sagittal proton-density-weighted fast spin-echo images of the knee obtained with a 16-channel (*ch*) flexible coil (left) and an eight-channel knee coil (right). SNR measured at three different regions of interest (red, green, and yellow circles) shows that the flexible coil can provide higher SNR than the knee coil.



Figure 15. Photographs show a 16-channel shoulder coil with an adjustable design. The top portion of the coil can be adjusted in height and angle to accommodate patients' different shoulder sizes and to optimize image quality. (Courtesy of Philips Healthcare.)

MRI (55) as well as to reduce RF power deposition (53). However, parallel imaging is subject to reduced SNR and potential image artifacts (56).

SNR in parallel imaging is given by the following:

$$SNR_p = SNR_0 / (g\sqrt{R}),$$

where SNR_0 is SNR without parallel imaging, g is the geometric factor (g factor), and R is the acceleration factor (57–59). The acceleration factor is the reduction factor in the phase-encoding steps, which also equals the reduction in imaging time. The g factor is related to coil design and has a minimum (ideal) value of 1. It is spatially varying and depends on the acquisition param-

eters, such as acceleration factor, phase-encoding direction, and field of view. Often, the average g factor or maximum g factor is used to represent the parallel imaging performance of a coil under a given imaging condition.

Generally speaking, RF coils with a larger number of coil elements have lower g factors, providing better SNR and supporting higher acceleration factor (Fig 17A, 17B). More specifically, parallel imaging performance depends on the number of coil elements in the direction of acceleration, which has to be larger than or equal to the acceleration factor for proper performance of parallel imaging. For a given phased-array coil, parallel imaging performance varies with the direction of acceleration, as

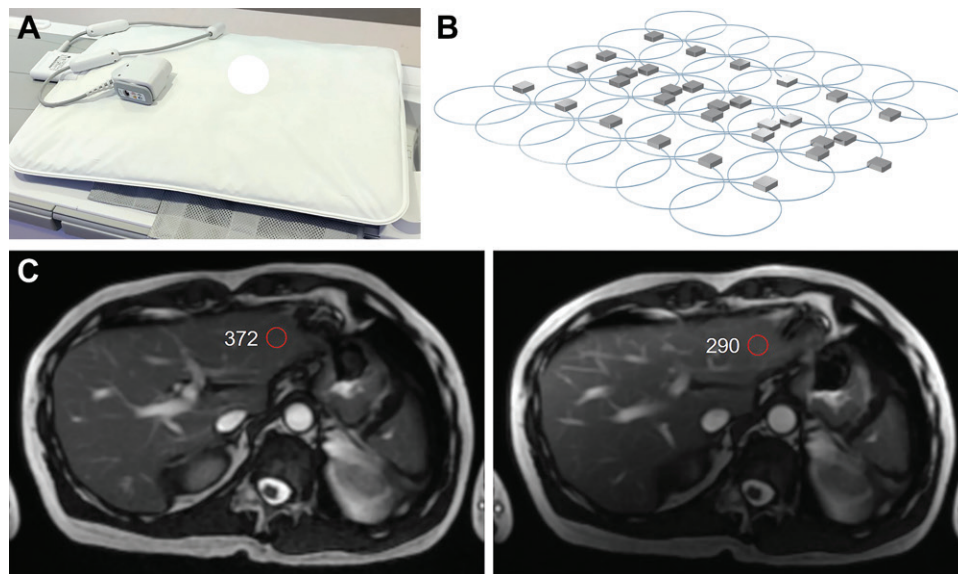


Figure 16. (A) Photograph shows a 30-channel linked-resonator anterior array coil. (B) Diagram shows its coil elements. (Courtesy of GE Healthcare.) (C) Abdomen images obtained with a breath-hold fast imaging employing steady-state acquisition (FIESTA) sequence using the linked-resonator coil (left) and a regular anterior array coil (right). The linked-resonator coil provides slightly higher SNR in the anterior region (red circle) and much stronger signal in the posterior region. This is attributed to the fact that the linked-resonator coil is very flexible and closely conforms to the body contour, allowing the coil to be closer to the body on the lateral sides.

the number of coil elements changes with direction (Fig 17C, 17D). Since SNR varies as follows:

$$1/(g\sqrt{R}),$$

it decreases when parallel imaging is used ($R > 1$).

One common mistake made in MRI protocols is to use parallel imaging to shorten imaging time while applying signal averaging to increase SNR. Since parallel imaging decreases SNR by $g\sqrt{R}$ but signal averaging increases SNR by \sqrt{N} , where N is the number of averages, the combined SNR varies as follows:

$$\sqrt{N}/(g\sqrt{R}).$$

For example, if N equals R , the imaging time will be the same as without parallel imaging and averaging, but the SNR will be lower by the factor g .

One situation in which it is beneficial to combine parallel imaging with signal averaging is when parallel imaging is used primarily to reduce image distortion in EPI-based sequences (55). Motion artifact reduction is another reason to combine signal averaging with parallel imaging. Although signal averaging can reduce motion artifacts, it increases imaging time and the chance of patient movement during the acquisition. On the other hand, parallel imaging reduces imaging time and may reduce or prevent patient movement (eg, by enabling breath holding). How to balance parallel imaging versus signal averaging in relationship to motion depends on specific applications and is an interesting topic to explore.

Similar to parallel imaging, the recently available simultaneous multislice (SMS) techniques (60) also require use of phased-array coils. The early implementation of SMS requires receive coils with elements distributed in the section direction. With development of techniques such as controlled aliasing in parallel imaging results in higher acceleration (CAIPIRINHA) (61) and blipped controlled aliasing in parallel imaging (CAIPI) (62), section separation can rely on coil sensitivities along the in-plane phase-encoding direction, relaxing the requirement for coil elements in the section direction and enabling a thinner gap between sections. A safety concern in SMS is that the SMS excitation pulse may increase RF power (60). Techniques such as power independent of number of sections (PINS) (63) and SMS excitation using parallel transmission (SMS-pTX) (64) have been developed to reduce the associated RF power.

RF Coil Signal Uniformity Correction.—Signal uniformity correction techniques such as surface coil intensity correction and preacquisition correction have been used to improve the signal uniformity of phased-array coils (Table) (65–67). Surface coil intensity correction filters the images by decreasing the signal intensity near the coil, while preacquisition correction uses information from a calibration acquisition to reduce signal nonuniformity (Fig 18A). However, uniformity correction may itself create problems if not used

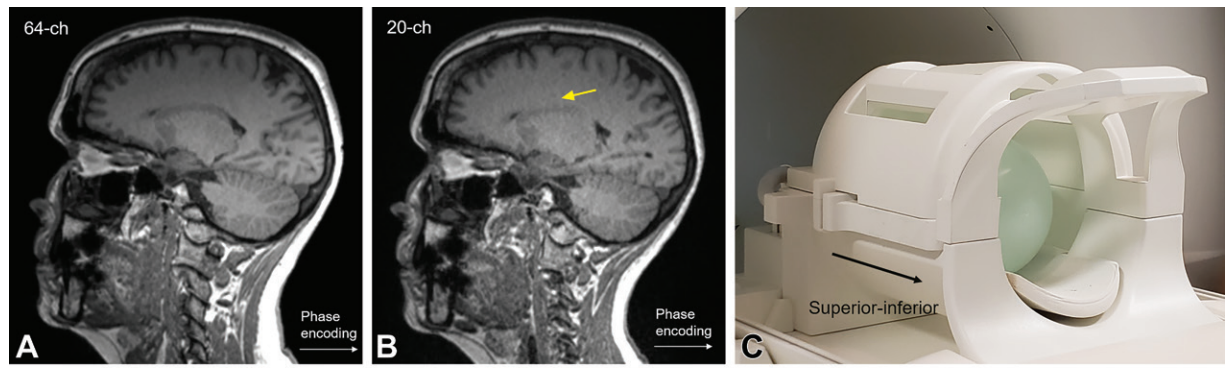


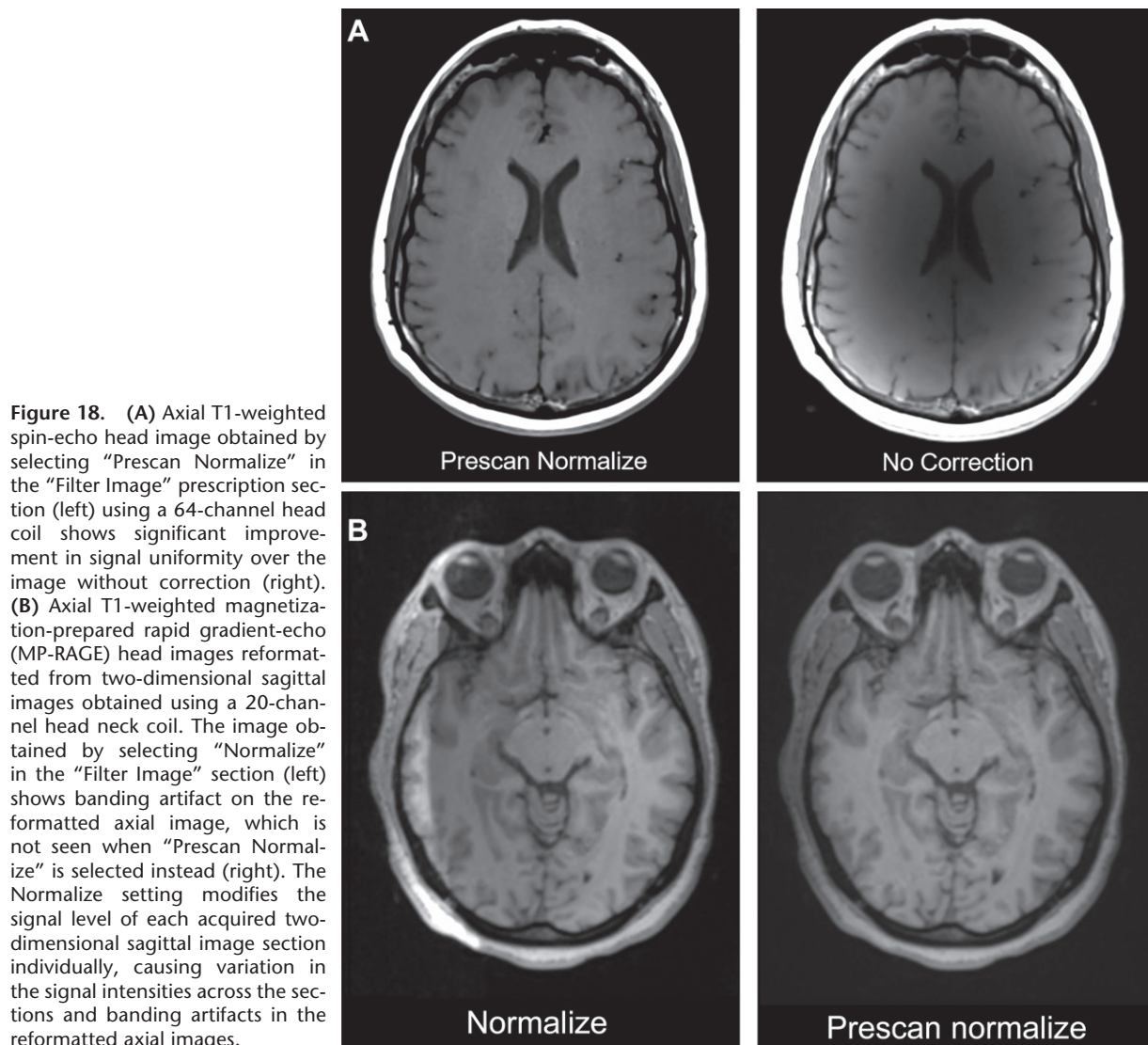
Figure 17. (A, B) Sagittal head images obtained with a T1-weighted magnetization-prepared rapid gradient-echo (MP-RAGE) sequence and generalized autocalibrating partial parallel acquisition (GRAPPA) ($R = 4$) using a 64-channel (*ch*) head coil (A) and a 20-channel head coil (B) at 3 T. Image parameters include repetition time (TR) = 1650 msec, echo time (TE) = 2.34 msec, inversion time (TI) = 962 msec, field of view (FOV) = 25 cm, matrix size = 256×256 , and “Prescan Normalize” selected. Compared with the 64-channel coil image, the 20-channel coil image shows obvious artifacts (arrow) and noise. (C, D) Photograph of a 16-channel head neck coil (C) and phantom images obtained using a gradient-echo sequence with GRAPPA ($R = 3$) (D) and phase encoding in the anterior-posterior direction (left) and superior-inferior direction (right). Image parameters include TR = 100 msec, TE = 10 msec, FOV = 25 cm, and matrix size = 256×256 . As parallel imaging takes place in the phase-encoding direction, the right image suffers from artifacts (arrows) and higher noise due to insufficient coil elements (only two) in the superior-inferior direction.

RF Coil Signal Uniformity Correction Techniques and Their Nomenclature from Some MRI Vendors		
Vendor, Mechanism, and Pros and Cons	Surface Coil Intensity Correction	Preacquisition Correction
GE Healthcare	SCIC	PURE
Siemens Healthineers	Normalize	Prescan Normalize
Philips Healthcare	Homogeneity Correction, Classic	CLEAR
Mechanism	Applies a postprocessing filter to the reconstructed image	Reduces coil nonuniformity by using a calibration acquired in a prior acquisition or during the adjustment measurement of the acquisition
Pros	Does not require a calibration acquisition	Based on the coil sensitivity profile May provide more accurate normalization
Cons	For two-dimensional acquisition, different filters may be applied to different imaging sections, leading to banding artifact in images reformatted to the orthogonal planes	PURE and CLEAR require a calibration acquisition that increases acquisition time and are susceptible to patient motion between the calibration acquisition and regular acquisition

Note.—CLEAR = constant level appearance, PURE = phased-array uniformity enhancement.

properly, as illustrated in Figure 18B. Moreover, care should be taken if signal uniformity correction is used in quantitative measurements such as functional MRI, diffusion coefficient mapping, and T2 mapping, as signal intensity will be modified (68). For example, if preacquisition correction is used in a dynamic contrast-enhanced study, it should be applied uniformly over all the dynamic series.

Coil Orientation.—The signal sensitivity of a surface coil varies with its orientation to the static magnetic field B_0 . If a surface coil loop is perpendicular to the B_0 field, the signal is nulled (Fig 19). Since a phased-array coil is composed of surface coil elements, it is also affected by its orientation to B_0 . For coils that do not have a fixed orientation in the MRI machine, such as



general-purpose flexible coils, improper coil orientation may degrade image quality.

Practical Considerations.—Practical considerations include choosing a coil for an MRI examination and the question of how many elements are sufficient.

The coil should match the size, shape, and field of view coverage of the imaged anatomy to optimize SNR. It would be desirable to use a dedicated coil, but if its size does not fit the patient, a suitable flexible coil may be used as an alternative.

Generally speaking, a larger number of coil elements increases SNR near the coil and also improves parallel imaging performance if the body resistance is larger than the coil resistance (as discussed under “Coil Designs” in the section on basic principles). There have been reports of a 96-channel head coil (33) and a 128-channel cardiac coil (69). Owing to manufacturing difficulties, coil cost, and system

channel compatibility, current clinical coils typically have 64 or fewer channels, with most coils having eight to 32 channels.

RF Coil Problems and Image Artifacts

The ability to correctly identify RF coil problems and distinguish them from other problems with image artifacts resembling those of RF coil problems allows effective handling of the problems and efficient clinical MRI operation.

RF Coil Problems and Associated Image Artifacts

RF coil problems may be identified from their associated image artifacts.

Failure of Coil or Coil Element.—Failure of a surface coil or an element in an array coil to detect MRI signal may be caused by malfunctioned electronic circuitry or a damaged cable or connector (Fig 20). As mentioned earlier, RF decoupling

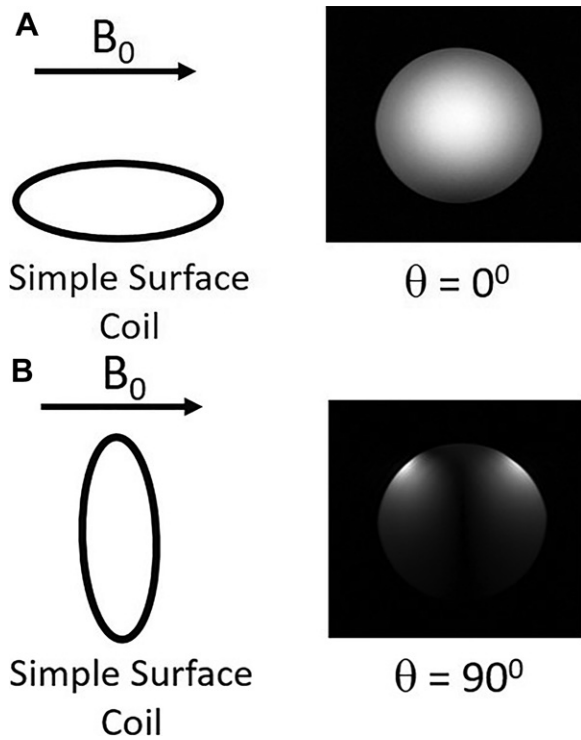


Figure 19. For a simple surface coil at an angle θ to the static magnetic field B_0 , signal varies as $\cos(\theta)$. The coil signal is strongest when $\theta = 0^\circ$ (A) and weakest when $\theta = 90^\circ$ (B).

failure is also a possible cause of coil signal loss (Fig 11). For a surface coil or coils with few elements, signal loss problems can be easily noticed (Fig 20B). However, as phased-array coils with a large number of elements are becoming common, it may be difficult to recognize signal loss in just one or two coil elements in routine clinical imaging, especially since it often will not show up as a dark spot because of uniformity correction. Phantom testing is needed to reveal the problem, as discussed in the section on quality control.

Failed or Poor Coil Connection to Imaging

Unit.—The connector of an RF coil needs to be securely plugged into the imaging unit for proper coil functioning (Fig 21A). A failed or poor coil connection is a common cause of coil problems, leading to failure to image, signal loss, or image artifacts (Fig 21B, 21C). Often, the only needed action for a suspected coil problem is to unplug and replug the connector to establish a proper coil connection. When checking for a coil connection problem, it is beneficial to also visually inspect the connector for any damage to the metal pins.

Other Problems with Image Artifacts Resembling Those of RF Coil Problems

Sometimes, MRI artifacts resemble those caused by an RF coil but actually have a different origin. The ability to distinguish these from coil problems

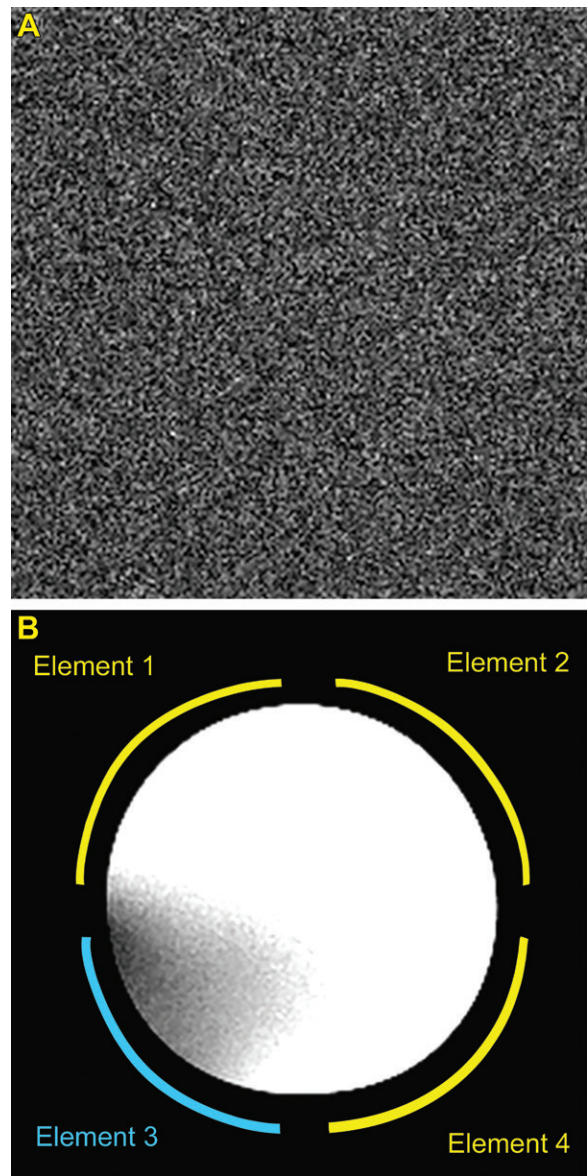


Figure 20. (A) Image shows absence of signal from a malfunctioned surface coil. (B) Image shows signal loss near malfunctioned coil element 3 of a phased-array coil.

will avoid unnecessary checking or changing of the coil or substituting it with a less desirable coil.

Fat Saturation Failure.—Fat saturation failure may sometimes resemble signal loss due to coil malfunction, but these two types of artifacts actually display different patterns (Figs 22, 23), which can be made use of to distinguish fat saturation failure from a coil problem.

RF Interference.—RF interference artifact appears as a bright line along the phase-encoding direction on an image. It may be misinterpreted as being caused by an RF coil (Fig 24). However, a broken coil typically shows much more random injection of noise throughout the image due to arcing.

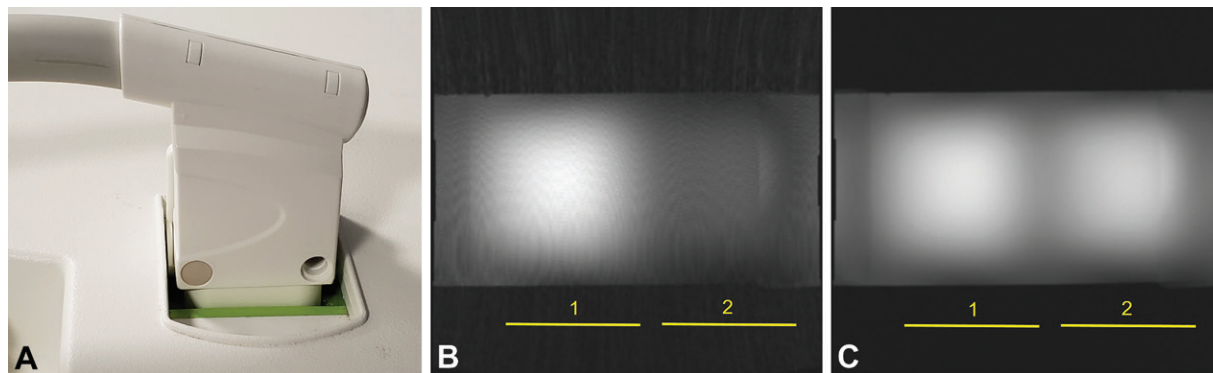


Figure 21. (A) Photograph shows an RF coil connector. (B) Phantom image shows an example of poor coil connection, which causes complete signal loss from coil element 2 and streak artifacts over the entire image. (C) Phantom image after the coil was properly reconnected to the imaging unit shows normal signal.

Signal Overflow.—Signal overflow artifacts have the appearance of signal saturation or bright background with altered image contrast, which cannot be overcome by adjusting the display window level (Fig 25). Mitigations of the problem include readjusting the receiver gain and modifying parameters to reduce signal (eg, decreasing section thickness).

Quality Control of RF Coils

Quality control of RF coils is important to ensure proper functioning of the coils to provide consistent image quality and avoid coil problems that may affect image evaluation or interrupt patient imaging. Routine RF coil quality control is also required in the accreditation program of the American College of Radiology (ACR).

RF coil quality control is performed by (a) visually inspecting the coil (including cables and connectors) to ensure its physical integrity and (b) phantom testing to evaluate the imaging performance of the coil. Phantom imaging is more sensitive than in vivo imaging in detecting coil problems. It is important to detect subtle coil problems, since signal loss in a couple of bad coil elements degrades image quality in the areas near those elements and may also affect overall imaging performance in parallel imaging, which relies on the proper signal profiles from individual coil elements. Besides, it is better to recognize a coil problem early than after it worsens with more malfunctioned coil elements.

While the ACR guideline (70) recommends checking all coils at least annually, it is beneficial to check them more often, especially frequently used coils and flexible coils. Preventive maintenance conducted by system manufacturers often does not include checking of all RF coils.

RF Coil Phantom Testing Methods

A phantom imaging test should be conducted using dedicated phantoms and phantom holders



Figure 22. (A) Sagittal image of the tibia shows local signal loss in both water and fat (arrow), caused by a defective coil element of an extremity phased-array coil. (B) Image of the forearm with fat saturation failure shows that fat signal is not properly suppressed, but water signal is suppressed instead (arrow).

specified by the coil or system manufacturer (Fig 26). Techniques that alter image signal and noise values—such as filters, uniformity correction, and parallel imaging—should not be used (68). The only exception is when a phased-array head coil is used in the ACR phantom quality control program, for which the uniformity correction technique is needed to satisfy the ACR signal uniformity requirement (70). There are different approaches to conducting phantom testing of RF coils. In this section, three commonly used methods are discussed (70–75).

Quantitative Signal and Noise Evaluation of an Image Section.

—This method is designed for single surface coils and volume coils but may also be extended for use in phased-array coils (70,75). Quantitative measurements are

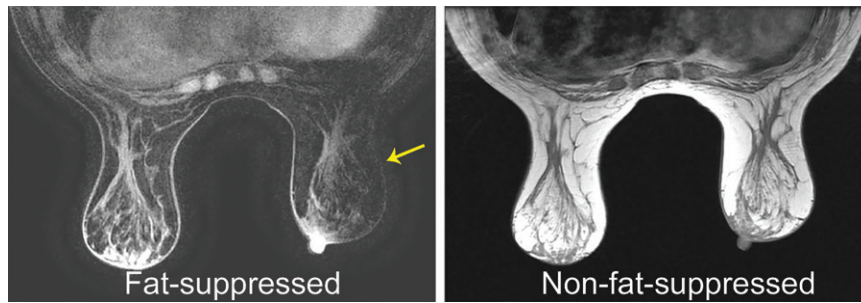


Figure 23. Images from a breast MRI examination at 3 T. Left: Fat-saturated image shows a region void of both water and fat signal (arrow), caused by erroneously suppressed water signal due to local field inhomogeneity. A way to distinguish this from a coil problem is to look at the corresponding non-fat-suppressed image (right): since the non-fat-suppressed image shows no signal loss in the same region, this implies that the artifact is caused by fat suppression failure and not a coil problem.

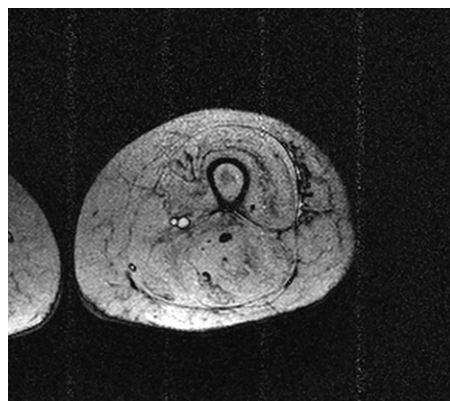


Figure 24. Axial image of the thigh obtained using a flexible extremity coil at 1.5 T shows RF interference artifact. The artifact was initially suspected to be caused by a coil problem. The MRI examination then switched to use of the imaging unit body coil. Although the artifact was not seen with the body coil, the SNR was much lower. Phantom tests later revealed that a power injector (turned off but plugged into a wall outlet) inside the MRI unit room was the actual cause of the artifact. The extremity coil picked up the RF interference from the power injector, but the body coil was not sensitive enough to do so.

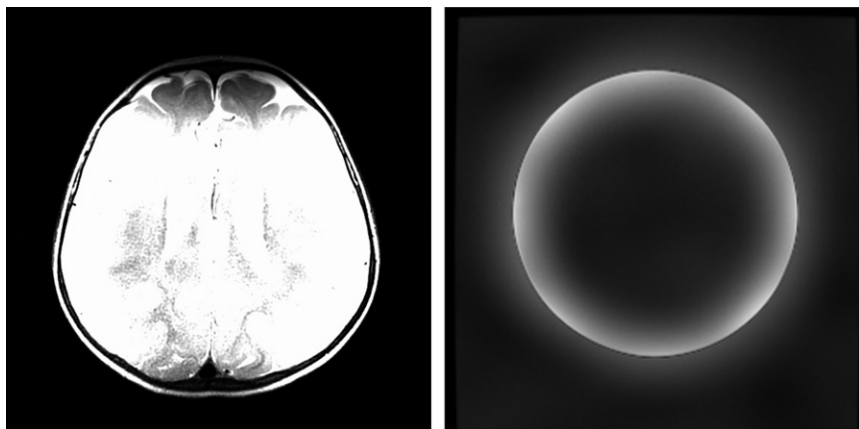


Figure 25. Examples of signal overflow artifact. Left: Head image shows the artifact as signal saturation. Right: Phantom image shows the artifact as bright background with altered image contrast.

made on an image near the center of the coil in the plane most often used clinically (Fig 27). For some phased-array coils, multiple section measurements are needed to cover all of the coil elements. However, prescribing appropriate section locations may not be easy, as the coil element location information is often unavailable to users. Another disadvantage with this method

is that a signal problem with a coil element may be obscured by the signal from other coil elements, especially for coils with a large number of elements (Fig 28).

SNR Evaluation of Images from Individual Coil Elements.—This method measures SNR from the images of each coil element of a phased-array coil



Figure 26. Photograph shows testing of an RF coil using the dedicated phantom and phantom holder specified by the MRI system manufacturer.



According to the ACR approach, mean SNR = mean signal in phantom/background noise. “Mean signal in phantom” is the signal magnitude (large red circle) measured from a region-of-interest that covers most of the cross-sectional area (> 75%) of the phantom.

“Background noise” S_{air} is the standard deviation from the background air measured in the frequency encoding direction. In this example, $S_{\text{air}} = \sqrt{\sigma_1^2 + \sigma_2^2}$, where σ_1 and σ_2 are standard deviation measured from the two green rectangles. Likewise, maximum (minimum) SNR = maximum (minimum) signal in phantom/background noise. “Maximum signal” and “minimum signal” are signal magnitudes (small red circles) measured from a small region (eg, 1 cm²) placed at the positions of highest and lowest signal in the phantom respectively. For a volume coil, percent image uniformity = $100 \times (1 - \frac{\text{maximum signal} - \text{minimum signal}}{\text{maximum signal} + \text{minimum signal}})$ and

$$\text{percent signal ghosting} = 100 \times \left| \frac{(\text{left} + \text{right}) - (\text{top} + \text{bottom})}{2 \times \text{mean signal}} \right| \text{ where (left, right) and (top, bottom) are signal magnitudes measured in the green boxes and yellow boxes respectively.}$$

Figure 27. Quantitative signal and noise evaluations performed on a phantom for a birdcage head coil.

to make sure each element functions properly (Fig 29) (68). This method requires the ability of the MRI system to reconstruct images for individual coil elements, which may not be available or accessible to users with some systems. As with the previous method, prescribing appropriate image sections to cover all of the coil elements may not be easy. In addition, manual SNR evaluation of individual elements can be time-consuming for phased-array coils with a large number of coil elements.

Using RF Coil Quality Assurance Tool Provided in MRI System.—Some MRI systems provide user access to RF coil quality assurance tools that perform automatic imaging and data analysis with predetermined pass-fail criteria (Fig 30). These tools measure SNR in specific regions of interest and may also evaluate the noise correlations among coil elements. They are generally sensitive and robust, able to pick up coil problems not easily detected with the other two methods, and particularly useful for coils with a large number

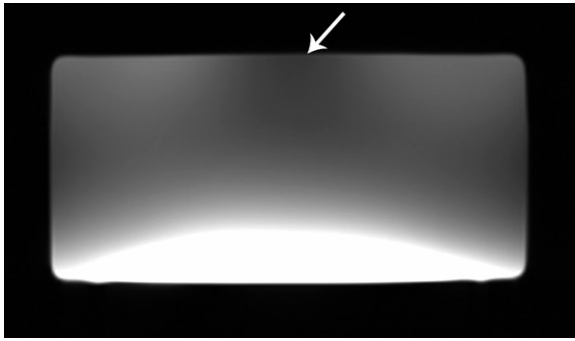


Figure 28. Image obtained from the neck portion of a 19-channel head and neck coil. One of the coil elements was defective (arrow), but the signal void was obscured by the signal from other coil elements and was not obvious. Measurements of maximum and mean SNR on this image did not reveal the problem. However, the coil problem was detected using the RF coil quality assurance tool of the MRI system.

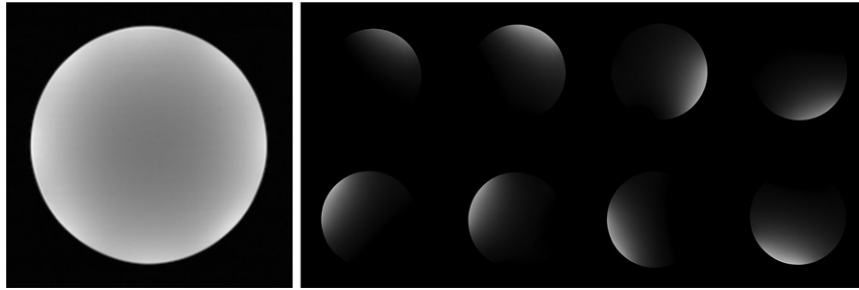


Figure 29. Composite image (left) and separate images reconstructed from the individual coil elements of an eight-channel head coil (photograph shown in Fig 4B) (right). By evaluating each element of a phased-array coil separately, a signal loss problem from a particular element will not be obscured by the signal from neighboring coil elements.

of elements. The disadvantage of RF coil quality assurance tools is that they may not be available or accessible in the MRI system.

Handling of RF Coils That Fail the Quality Control Test

The most common RF coil problem is signal loss or inhomogeneity caused by failure of one or more coil elements, as discussed in the section on RF coil problems. In other situations, a coil may fail to image owing to a damaged coil plug, opened circuitry, or a malfunctioned detuning circuit, in which case the MRI system may block the imaging. Damage to the coil casing or coil cable may be determined by visual inspection.

Because coil problems usually cannot be diagnosed or fixed by the users, the coil vendor or system manufacturer should be contacted to have the coil checked and repaired or replaced. Alternatively, the coil may be sent to a third-party company that provides RF coil repair services. An RF coil that fails the quality control test should not be used in patients to ensure their safety. Coils that fail often should be checked more frequently, and this may indicate the need to improve handling or storage of the coils.

Conclusion

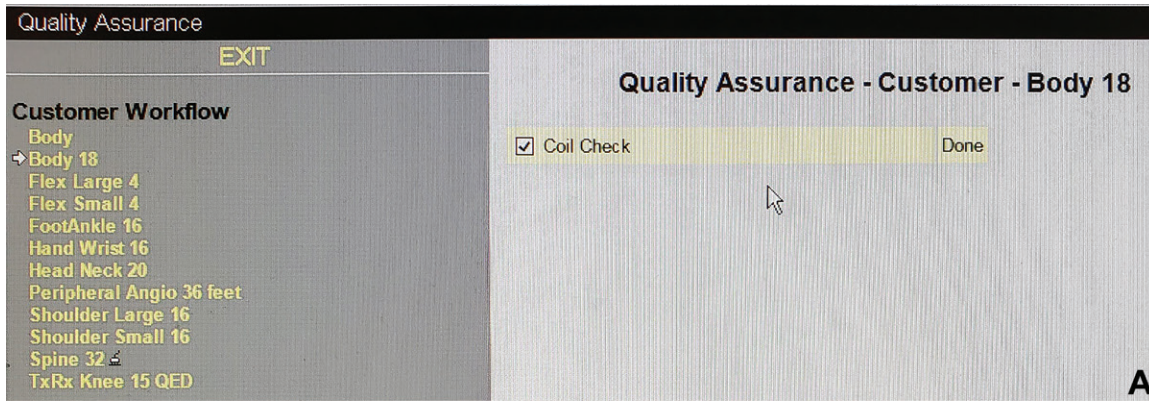
Knowledge of the basic principles and proper use of RF coils is needed to achieve optimal image quality and reduce RF heating risk. Correct iden-

tification of coil problems and proper coil quality control facilitate effective and efficient clinical MRI operation.

Acknowledgment.—The author would like to acknowledge Winfried A. Willinek, MD, GE Healthcare, and Philips Healthcare for commissioned illustrations.

References

1. Fujita H, Zheng T, Yang X, Finnerty MJ, Handa S. RF surface receive array coils: the art of an LC circuit. *J Magn Reson Imaging* 2013;38(1):12–25.
2. Haacke EM, Brown RW, Thompson MR, Venkatesan MR. *Magnetic Resonance Imaging: Physical Principles and Sequence Design*. New York, NY: Wiley-Liss, 1999; 4–6.
3. Kneeland JB, Hyde JS. High-resolution MR imaging with local coils. *Radiology* 1989;171(1):1–7.
4. Hayes CE, Axel L. Noise performance of surface coils for magnetic resonance imaging at 1.5 T. *Med Phys* 1985;12(5):604–607.
5. Roemer PB, Edelstein WA, Hayes CE, Souza SP, Mueller OM. The NMR phased array. *Magn Reson Med* 1990;16(2):192–225.
6. Hayes CE, Hattes N, Roemer PB. Volume imaging with MR phased arrays. *Magn Reson Med* 1991;18(2):309–319.
7. Gruber B, Froeling M, Leiner T, Klomp DWJ. RF coils: a practical guide for nonphysicists. *J Magn Reson Imaging* 2018;48(3):590–604.
8. Hoult DI, Lauterbur PC. The sensitivity of the zeugmatographic experiment involving human samples. *J Magn Reson* 1979;34(2):425–433.
9. Tropp J. The theory of the bird-cage resonator. *J Magn Reson* 1989;82(1):51–62.
10. Hayes CE, Edelstein WA, Schenck JF, Mueller OM, Eash M. An efficient, highly homogeneous radiofrequency coil for whole-body NMR imaging at 1.5T. *J Magn Reson* 1985;63(3):622–628.
11. Doty FD, Entzminger G Jr, Hauck CD, Staab JP. Practical aspects of birdcage coils. *J Magn Reson* 1999;138(1):144–154.



Quality Assurance

Coil Check Body_18 Success

Comments (0)

#	Timestamp	Comment
No comments for this function.		

Summary

	Status
098_Body_18_H_Tra	OK
098_Body_18_F_Tra	OK
098_Body_18_L_Sag	OK
098_Body_18_R_Sag	OK
Program Result	Success

Details

Protocol: 098_Body_18_H_Tra

Coil Info		
Coil ID	Serial Number	Part Number
Body_18	33028	10496530

Coil:

B11_B12_B13_B14_B15_B16_B21_B22_B23_B24_B25_B26_B31_B32_B33_B34_B35_B36

Signal

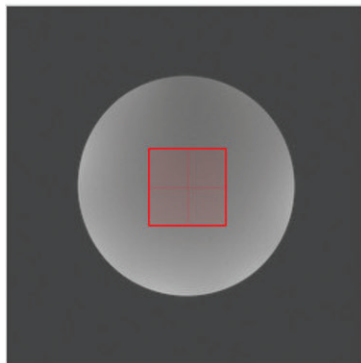


Figure 30. Example of an RF coil quality assurance tool that provides a specific imaging protocol for each coil (A) and its automatic image signal and noise analysis with predetermined passed-failed criteria (B).

12. Kraff O, Quick HH. Radiofrequency Coils for 7 Tesla MRI. *Top Magn Reson Imaging* 2019;28(3):145–158.
13. Rietsch SHG, Orzada S, Maderwald S, et al. 7T ultra-high field body MR imaging with an 8-channel transmit/32-channel receive radiofrequency coil array. *Med Phys* 2018;45(7):2978–2990.
14. Panych LP, Madore B. The physics of MRI safety. *J Magn Reson Imaging* 2018;47(1):28–43.
15. Glover GH, Hayes CE, Pelc NJ, et al. Comparison of linear and circular polarization for magnetic resonance imaging. *J Magn Reson* 1985;64(2):255–270.
16. Chen CN, Hoult DI, Sank VJ. Quadrature detection coils: a further $\sqrt{2}$ improvement in sensitivity. *J Magn Reson* 1983;54(2):324–327.
17. Hyde JS, Jesmanowicz A, Grist TM, Froncisz W, Kneeland JB. Quadrature detection surface coil. *Magn Reson Med* 1987;4(2):179–184.
18. Feng L, Chen V, Lakshmanan K, Yang YJ. The SENSE CTL Coil for 3T 8-Channel MRI Systems [abstr]. In: Proceedings of the 12th Meeting of the International Society for Magnetic Resonance in Medicine. Berkeley, Calif: International Society for Magnetic Resonance in Medicine, 2004.
19. Dietrich O, Reiser MF, Schoenberg SO. Artifacts in 3-T MRI: physical background and reduction strategies. *Eur J Radiol* 2008;65(1):29–35.
20. Willinek WA, Gieseke J, Kukuk GM, et al. Dual-source parallel radiofrequency excitation body MR imaging compared with standard MR imaging at 3.0 T: initial clinical experience. *Radiology* 2010;256(3):966–975.
21. Setsompop K, Wald LL, Alagappan V, et al. Parallel RF transmission with eight channels at 3 Tesla. *Magn Reson Med* 2006;56(5):1163–1171.
22. Brink WM, Gulani V, Webb AG. Clinical applications of dual-channel transmit MRI: a review. *J Magn Reson Imaging* 2015;42(4):855–869.
23. Kukuk GM, Gieseke J, Weber S, et al. Focal liver lesions at 3.0 T: lesion detectability and image quality with T2-weighted imaging by using conventional and dual-source parallel radiofrequency transmission. *Radiology* 2011;259(2):421–428.
24. Murbach M, Neufeld E, Cabot E, et al. Virtual population-based assessment of the impact of 3 tesla radiofrequency shimming and thermoregulation on safety and B1+ uniformity. *Magn Reson Med* 2016;76(3):986–997.
25. Childs AS, Malik SJ, O'Regan DP, Hajnal JV. Impact of number of channels on RF shimming at 3T. *MAGMA* 2013;26(4):401–410.
26. Reykowski A, Wright SM, Porter JR. Design of matching networks for low noise preamplifiers. *Magn Reson Med* 1995;33(6):848–852.
27. Edelstein WA, Hardy CJ, Mueller OM. Electronic decoupling of surface-coil receivers for NMR imaging and spectroscopy. *J Magn Reson* 1986;67(1):156–161.
28. Boskamp EB. Improved surface coil imaging in MR: decoupling of the excitation and receiver coils. *Radiology* 1985;157(2):449–452.
29. Bendall MR, Connelly A, McKendry JM. Elimination of coupling between cylindrical transmit coils and surface-receive coils for in vivo NMR. *Magn Reson Med* 1986;3(1):157–163.
30. Wang W, Zhurbenko V, Sánchez-Heredia JD, Ardenkjaer-Larsen JH. Three-element matching networks for receive-only MRI coil decoupling. *Magn Reson Med* 2021;85(1):544–550.
31. Haase A, Odoj F, von Kienlin M, et al. NMR probeheads for in vivo applications. *Concepts Magn Reson* 2000;12(6):361–388.
32. Hayes CE, Roemer PB. Noise correlations in data simultaneously acquired from multiple surface coil arrays. *Magn Reson Med* 1990;16(2):181–191.
33. Wiggins GC, Polimeni JR, Potthast A, Schmitt M, Alagappan V, Wald LL. 96-Channel receive-only head coil for 3 tesla: design optimization and evaluation. *Magn Reson Med* 2009;62(3):754–762.
34. Ohliger MA, Ledden P, McKenzie CA, Sodickson DK. Effects of inductive coupling on parallel MR image reconstructions. *Magn Reson Med* 2004;52(3):628–639.
35. Reykowski A, Saylor C, Duensing GR. Do we need pre-amplifier decoupling? [abstr]. In: Proceedings of the 19th Meeting of the International Society for Magnetic Resonance in Medicine. Berkeley, Calif: International Society for Magnetic Resonance in Medicine, 2011.
36. Findekle C, Lips O, Vernickel P, Leussler C, Duensing R. Preamp decoupling improves SNR and the earth is flat [abstr]. In: Proceedings of the 27th Meeting of the International Society for Magnetic Resonance in Medicine. Berkeley, Calif: International Society for Magnetic Resonance in Medicine, 2019.
37. Duensing R, Findekle C. Preamplifier decoupling: Theory & Practice [abstr]. In: Proceedings of the 29th Meeting of the International Society for Magnetic Resonance in Medicine. Berkeley, Calif: International Society for Magnetic Resonance in Medicine, 2021.
38. Peterson DM, Beck BL, Duensing GR, Fitzsimmons JR. Common mode signal rejection methods for MRI: reduction of cable shield currents for high static magnetic field systems. *Concepts Magn Reson Part B* 2003;19B(1):1–8.
39. Seeber DA, Jevtic J, Menon A. Floating shield current suppression trap. *Concepts Magn Reson Part B* 2003;21B(1):26–31.
40. Lemdiasov R, Venkatasubramanian A, Jegadeesan R. Estimating Electric Field and SAR in Tissue in the Proximity of RF Coils. In: Makarov SN, Noetscher GM, Nummenmaa A, eds. *Brain and Human Body Modeling 2020: Computational Human Models Presented at EMBC 2019 and the BRAIN Initiative 2019 Meeting*. Berlin, Germany: Springer, 2021.
41. Shellock FG. Radiofrequency energy-induced heating during MR procedures: a review. *J Magn Reson Imaging* 2000;12(1):30–36.
42. American College of Radiology. *ACR Manual on MR Safety*. Reston, Va: American College of Radiology, 2020.
43. Tsai LL, Grant AK, Mortelet KJ, Kung JW, Smith MP. A Practical Guide to MR Imaging Safety: What Radiologists Need to Know. *RadioGraphics* 2015;35(6):1722–1737.
44. Stormont R, Robb F, Lindsey S, et al. Reimagining flexible coil technology. *GESIGNAPULSE.com*. https://www.gesignapulse.com/signapulse/spring_2017/MobilePagedArticle.action?articleId=1160235#articleId1160235. Published 2017. Accessed December 2017.
45. Collick BD, Behzadnezhad B, Hurley SA, et al. Rapid development of application-specific flexible MRI receive coils. *Phys Med Biol* 2020;65(19):19NT01.
46. McGee KP, Stormont RS, Lindsay SA, et al. Characterization and evaluation of a flexible MRI receive coil array for radiation therapy MR treatment planning using highly decoupled RF circuits. *Phys Med Biol* 2018;63(8):08NT02.
47. Truong TK, Darnell D, Song AW. Integrated RF/shim coil array for parallel reception and localized B0 shimming in the human brain. *Neuroimage* 2014;103:235–240.
48. Stockmann JP, Witzel T, Keil B, et al. A 32-channel combined RF and B0 shim array for 3T brain imaging. *Magn Reson Med* 2016;75(1):441–451.
49. Keil MR, Rothard J, Hayes C. BioMatrix Tuners: CoilShim. *MAGNETOM Vida special issue: Head and Neck Imaging Clinical*. http://clinical-mri.com/wp-content/uploads/2017/03/BioMatrix_CoilShim_MAGNETOM_Vida.pdf. Accessed December 2017.
50. Griswold MA, Jakob PM, Heidemann RM, et al. Generalized autocalibrating partially parallel acquisitions (GRAPPA). *Magn Reson Med* 2002;47(6):1202–1210.
51. Pruessmann KP, Weiger M, Scheidegger MB, Boesiger P. SENSE: sensitivity encoding for fast MRI. *Magn Reson Med* 1999;42(5):952–962.
52. Keil B, Blau JN, Biber S, et al. A 64-channel 3T array coil for accelerated brain MRI. *Magn Reson Med* 2013;70(1):248–258.
53. Deshmane A, Gulani V, Griswold MA, Seiberlich N. Parallel MR imaging. *J Magn Reson Imaging* 2012;36(1):55–72.
54. Glockner JF, Hu HH, Stanley DW, Angelos L, King K. Parallel MR imaging: a user's guide. *RadioGraphics* 2005;25(5):1279–1297.
55. Schmidt CF, Degonda N, Luechinger R, Henke K, Boesiger P. Sensitivity-encoded (SENSE) echo planar fMRI at 3T in the medial temporal lobe. *Neuroimage* 2005;25(2):625–641.

56. Noël P, Bammer R, Reinhold C, Haider MA. Parallel imaging artifacts in body magnetic resonance imaging. *Can Assoc Radiol J* 2009;60(2):91–98.
57. Robson PM, Grant AK, Madhuranthakam AJ, Lattanzi R, Sodickson DK, McKenzie CA. Comprehensive quantification of signal-to-noise ratio and g-factor for image-based and k-space-based parallel imaging reconstructions. *Magn Reson Med* 2008;60(4):895–907.
58. Reeder SB, Wintersperger BJ, Dietrich O, et al. Practical approaches to the evaluation of signal-to-noise ratio performance with parallel imaging: application with cardiac imaging and a 32-channel cardiac coil. *Magn Reson Med* 2005;54(3):748–754.
59. Breuer FA, Kannengiesser SA, Blaimer M, Seiberlich N, Jakob PM, Griswold MA. General formulation for quantitative g-factor calculation in GRAPPA reconstructions. *Magn Reson Med* 2009;62(3):739–746.
60. Barth M, Breuer F, Koopmans PJ, Norris DG, Poser BA. Simultaneous multislice (SMS) imaging techniques. *Magn Reson Med* 2016;75(1):63–81.
61. Breuer FA, Blaimer M, Heidemann RM, Mueller MF, Griswold MA, Jakob PM. Controlled aliasing in parallel imaging results in higher acceleration (CAIPIRINHA) for multi-slice imaging. *Magn Reson Med* 2005;53(3):684–691.
62. Setsompop K, Gagoski BA, Polimeni JR, Witzel T, Wedeen VJ, Wald LL. Blipped-controlled aliasing in parallel imaging for simultaneous multislice echo planar imaging with reduced g-factor penalty. *Magn Reson Med* 2012;67(5):1210–1224.
63. Norris DG, Koopmans PJ, Boyacıoğlu R, Barth M. Power Independent of Number of Slices (PINS) radiofrequency pulses for low-power simultaneous multislice excitation. *Magn Reson Med* 2011;66(5):1234–1240.
64. Poser BA, Anderson RJ, Guérin B, et al. Simultaneous multislice excitation by parallel transmission. *Magn Reson Med* 2014;71(4):1416–1427.
65. Gelber ND, Ragland RL, Knorr JR. Surface coil MR imaging: utility of image intensity correction filter. *AJR Am J Roentgenol* 1994;162(3):695–697.
66. Vovk U, Pernus F, Likar B. A review of methods for correction of intensity inhomogeneity in MRI. *IEEE Trans Med Imaging* 2007;26(3):405–421.
67. Ganzetti M, Wenderoth N, Mantini D. Quantitative Evaluation of Intensity Inhomogeneity Correction Methods for Structural MR Brain Images. *Neuroinformatics* 2016;14(1):5–21.
68. Dietrich O, Raya JG, Reeder SB, Reiser MF, Schoenberg SO. Measurement of signal-to-noise ratios in MR images: influence of multichannel coils, parallel imaging, and reconstruction filters. *J Magn Reson Imaging* 2007;26(2):375–385.
69. Schmitt M, Potthast A, Sosnovik DE, et al. A 128-channel receive-only cardiac coil for highly accelerated cardiac MRI at 3 Tesla. *Magn Reson Med* 2008;59(6):1431–1439.
70. American College of Radiology. *Magnetic Resonance Imaging Quality Control Manual*. Reston, Va: American College of Radiology, 2015.
71. National Electrical Manufacturers Association. *NEMA-MS-1: Determination of SNR in Diagnostic Magnetic Resonance Images*. Rosslyn, Va: National Electrical Manufacturers Association, 2008.
72. National Electrical Manufacturers Association. *NEMA-MS-3: Determination of Image Uniformity in Diagnostic Magnetic Resonance Images*. Rosslyn, Va: National Electrical Manufacturers Association, 2008.
73. National Electrical Manufacturers Association. *NEMA-MS-6: Determination of Signal-to-Noise Ratio and Image Uniformity for Single-channel, Non-volume Coils in Diagnostic Magnetic Resonance Imaging (MRI)*. Rosslyn, Va: National Electrical Manufacturers Association, 2008.
74. National Electrical Manufacturers Association. *NEMA-MS-9: Characterization of Phase Array Coils for Diagnostic Magnetic Resonance Images*. Rosslyn, Va: National Electrical Manufacturers Association, 2008.
75. Constantinides CD, Atalar E, McVeigh ER. Signal-to-noise measurements in magnitude images from NMR phased arrays. *Magn Reson Med* 1997;38(5):852–857.